Response of Historic Masonry Structures to Tectonic Ground Displacements

M. Loli, I. Anastasopoulos, G. Gazetas
National technical University of Athens, Greece

S. Cattari, S. Degli Abbati, S. Lagomarsino
University of Genoa, Italy

15 WCEE
LISBOA 2012

SUMMARY:
The response of historic masonry buildings subjected to tectonically induced ground distress is studied through analysis of a simple yet representative soil–foundation–masonry wall system. A hybrid methodology is adopted to rigorously account for the multiple response nonlinearities, combining a validated 3D FE model for simulation of fault rupture–soil–foundation – structureinteraction with a well-established nonlinear macro-element model for simulation of the response of masonry panels. It comprises two steps: (a) calculation of the foundation displacements due to interaction with the fault rupture assuming elastic superstructure response, and (b) analysis of the nonlinear response of the masonry wall subjected to the foundation displacements of the first step, to predict its consequent damage. Following a sensitivity analysis of the effect of the exact location of the structure with respect to the fault, the paper discusses several characteristic mechanisms of response to reverse fault rupture and assesses the associated masonry damage.

Keywords: Historic Structures; Permanent Ground Displacements; Nonlinear Soil–Structure Interaction

1. INTRODUCTION

Besides being the generation source of earthquakes, tectonic faults may also directly affect surface structures by means of permanent ground displacements. This is likely to be the case in large magnitude and/or shallow earthquakes, when the causative fault may propagate all the way to the ground surface and outcrop causing its permanent deformation thereby imposing significant distress to overlying structures. As a matter of fact, a number of seismic events during past years, for instance the 1999 Kocaeli earthquake in Turkey; the 1999 Düzce earthquake also in Turkey; the 1999 Chi-Chi earthquake in Taiwan; and the 2008 Wenchuan earthquake in China , have been characterized by extensive damage to structures due to the emergence of the fault rupture directly underneath them.

Although the response of historic structures subjected to tectonic loads has not been explicitly addressed in the literature, it is evident that, as well as most other structure types, monuments can be particularly susceptible to such permanent ground deformations. **Figure 1a** shows the only, to the authors' knowledge, documented failure of a monument due to interaction with a rupturing fault. This took place in Denizevler (Turkey), when during the Kocaeli 1999 earthquake the causative fault outcropped and the surface rupture crossed the mosque depicted in the figure. Anastasopoulos & Gazetas [2007] interpreted the failure of the mosque anticipating the fault–soil–structure interaction mechanism shown in the schematic of **Figure 1b**.

It is essential to highlight that given their significantly longer lifetime expectancy and in many cases their relatively large size, monuments are more likely than most other structures to experience such tectonic hazards. Moreover, even if modern constructions can be designed to withstand or relocated to avoid active faults that are already known, this is presumably inapplicable to (already existing) monuments. Hence, it is necessary to account for faulting-induced loading in the seismic assessment and retrofit of historic structures in seismically active areas. Being part of a major European project which deals with the seismic protection of monuments in the Mediterranean, this paper presents results from an ongoing research initiative which aims at developing a methodology for the analysis, assessment and mitigation of tectonic risk for historic masonry structures.

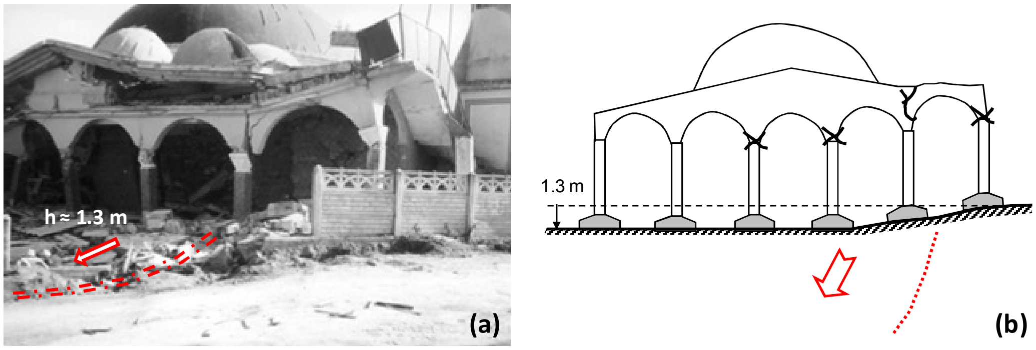

Figure 1. Mosque collapse in Denizevler (Turkey) due to permanent tectonic deformation of the soil surface: (a) photograph of the Mosque showing the differential settlement of the un-scarped ground surface and the distress of its superstructure, and (b) sketch of plausible failure mechanism [Anastasopoulos & Gazetas, 2007].

2. DEFINITION OF THE FAUT–STRUCTURE INTERACTION POBLEM

Figure 2 defines schematically the geometry of the studied problem. A very simplified, yet representative, single wall structure model is herein employed to study the vulnerability of old masonry buildings under permanent ground displacements due to interaction with a reverse fault rupture. Its geometry is inspired by the well known "Door-Wall" used in the large scale experiments reported by Magenes et al. [1995]. The structure is made of unreinforced masonry, consisting of solid fired-clay bricks and mixed hydraulic mortar, representing typical old urban construction in many European cities. It carries the dead weight of two floors (248.4 kN and 236.8 kN) through three shear wall elements, which are supported by isolated footings (Footings 1-3).

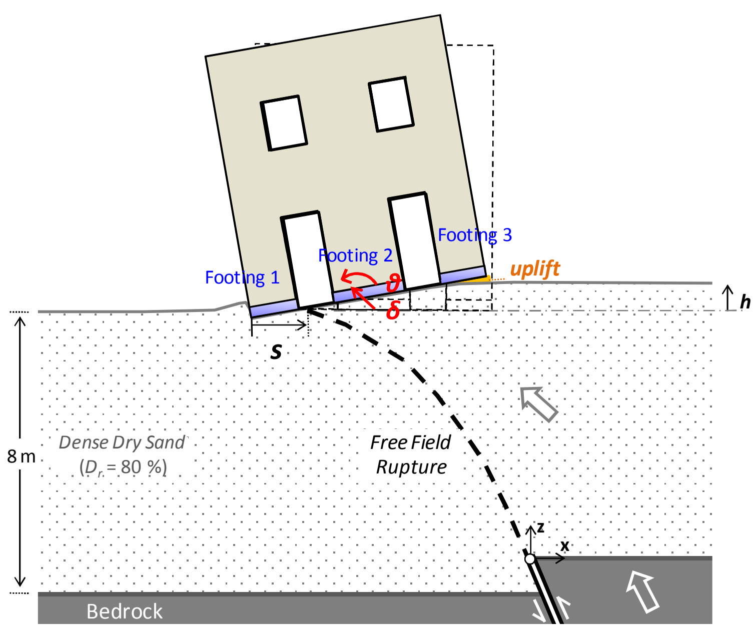

Figure 2. Definition of the studied problem: geometry and key parameters.

The masonry structure is founded upon an 8 m deep layer of dense dry sand and tectonic displacement of vertical throw h is imposed at the underlying bedrock. For the case of thrust faulting, which is investigated herein, the displaced block (hanging-wall) moves upwards. If the structure did not exist (i.e., in free-field conditions), fault deformation would localize upon a rupture plane as indicated by the dashed line. The presence of the structure, however, is expected to more or less modify the rupture path. As a result, the foundation–structure system is bound to experience some permanent displacements (δ, θ). Past studies on the interaction foundation–structure systems with dip-slip fault ruptures suggest that the exact response would significantly depend on the position of the structure with respect to the fault. This parameter is here quantified by distance s, which is the horizontal distance between the left (footwall-side) corner of the structure and the point where the free field rupture plane would cross the foundation level.

3. METHODOLOGY

A hybrid methodology is adopted to rigorously account for the multiple nonlinearities in the response of the rupturing soil and the distressed masonry structure, combining an experimentally validated 3D FE model for simulation of fault rupture–soil–foundation interaction with a well-established nonlinear macro-element model for simulation of the response of masonry panels. It comprises two steps: (a) calculation of the foundation displacements resulting from their interaction with the fault rupture assuming elastic superstructural response, and (b) analysis of the nonlinear response of the masonry wall subjected to the foundation displacements of the first step, to predict its consequent damage.

3.1. Step 1: 3D FE analysis of Fault Rupture–Soil–Foundation–Structure Interaction

Former studies have shown that the finite element (FE) method can quite accurately simulate the phenomenon of fault rupture propagation in the free field [e.g., Bray et al., 1994; Anastasopoulos et al., 2007] as well as its interaction with foundations [e.g., Anastasopoulos et al., 2009; Loli et al., 2011]. 3D FE modelling is required to realistically simulate the problem considered herein mainly due to the importance of footing shape effects. The FE code ABAQUS was utilized for this purpose and **Figure 3** depicts the adequately discretized FE mesh used in the analyses, also indicating the main modelling features and mesh characteristics.

The sand layer was modelled with 8-noded continuum elements, the nonlinear response of which was simulated according to the methodology of Anastasopoulos et al. [2007]. Mohr-Coulomb failure criterion is combined with isotropic strain softening, according to which the friction (φ) and dilation (ψ) angles reduce linearly with octahedral plastic shear strain γ_{oct} as follows:

$$\varphi;\psi = \left\{ \begin{array}{ll} \varphi_p - \frac{\varphi_p - \varphi_{cs}}{\gamma_f^{pl}} \gamma_{oct}^{pl} \ ; \ \psi_p \left(1 - \frac{\gamma_{oct}^{pl}}{\gamma_f^{pl}}\right) & , for \ \ 0 \leq \gamma_{oct}^{pl} < \gamma_f^{pl} \\ \varphi_{cs} \ ; \ 0 & , for \ \ \gamma_{oct}^{pl} \geq \gamma_f^{pl} \end{array} \right\} \quad (1)$$

where, φ_p and φ_{cs} the peak and critical state soil friction angles; ψ_p the peak dilation angle; and $\gamma_f^{\ P}$ the octahedral plastic shear strain at the end of softening. The dense sand layer of the specific problem was assumed to have the following properties: $\varphi_p = 40°$; $\psi_p = 10°$; $\varphi_{CS} = 32°$; $\varphi_p = 2°$; and $\gamma_f^{\ P} = 0.05$.

In contrast to the adequately realistic modelling of nonlinear soil response and failure, FE analyses reproduced the structural material behaviour rather crudely assuming elastic response of the masonry wall as well as the foundation (with a reduced Young's modulus value to consider cracked conditions). Therefore, although considered sufficient for the estimation of fault induced foundation movements, and subsequently for the estimation of the faulting-induced distress imposed onto the structure, FE results may not be utilized directly for the assessment of wall damage. The latter, is conducted in the second step, using sophisticated analysis of the masonry wall response, as described in the following section.

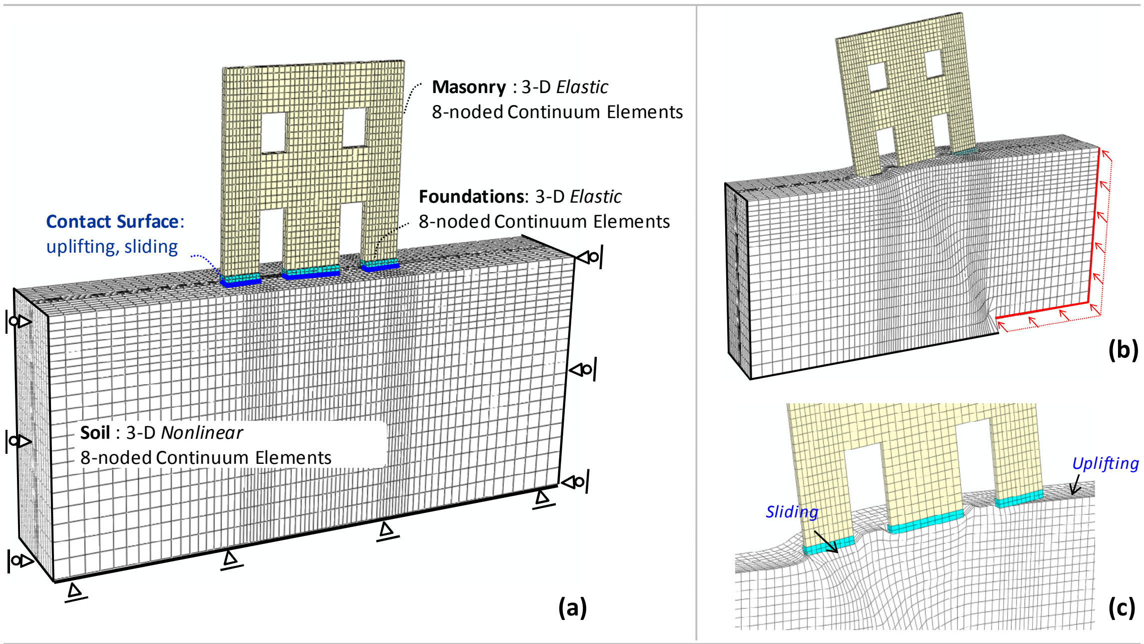

Figure 3. 3D FE mesh indicating material and surface contact modelling details and boundary conditions.

Loading was applied through consecutive steps: (i) geostatic stress; (ii) static load of the structure; and (iii) incremental fault displacement. During the first two steps the model boundaries were restrained according to the conditions illustrated in **Figure 3a**. Boundary conditions were then modified, so as to apply the fault displacement of the bedrock, moving the hanging wall side up-left with a dip angle of 60° (**Figure 3b**). It should be noted that the numerical analysis included a sensitivity study of the effect of the exact structure position with respect to the fault, by parametrically varying parameter s, aiming at enveloping all the possible mechanisms of interaction. Moreover, as shown in **Figure 3c**, soil–foundation interface behaviour was found to greatly influence the response and was therefore realistically modelled, using a suitable interface allowing for sliding (with friction coefficient $\mu = 0.5$ to account for the rather rough interface between masonry and soil) and detachment (loss of contact at zero pressure).

3.2. Step 2: Equivalent Frame analysis of the nonlinear wall response

The Equivalent Frame method has been widely employed in the analysis of standard masonry wall structures thanks to its effectiveness in accurately predicting their response, provided that suitable constitutive relations are incorporated to account for the relevant attributes of nonlinear material behaviour, in addition to its computational efficiency. Implemented within the *Tremuri* software, originally developed at the University of Genoa starting from 2002 [Galasco et al., 2009], the Equivalent Frame method has been herein employed to study the response of the masonry wall subject to permanent displacements of its foundations, as the latter result due to interaction with the fault rupture in different positions of the structure.

The wall is discretized in a set of masonry panels connected by rigid nodes (**Figure 4**). The panels, which are deformable and undergo damage, are classified into two main types, the piers (the principal bearing elements carrying dead and seismic loads) and the spandrels (secondary horizontal elements providing coupling between the piers), which are connected with rigid elements.

Nonlinear pier behaviour is introduced using a well established macroelement model [Galasco et al., 2004] developed with respect to the continuous model formulated by Gambarotta & Lagomarsino [1997], whereby the two main modes of in-plane masonry failure, namely the bending–rocking response and the shear–sliding response, may be reproduced on the basis of mechanical assumptions. The model was appropriately modified to include the effect of the limited compressive strength of masonry as suggested by Penna [2002]. In a few words, the model takes into account, by means of internal variables, the development of tensile cracks at the piers corners (due to flexure) as well as the shear-sliding damage evolution, which controls the mechanisms of strength deterioration (softening) and stiffness degradation.

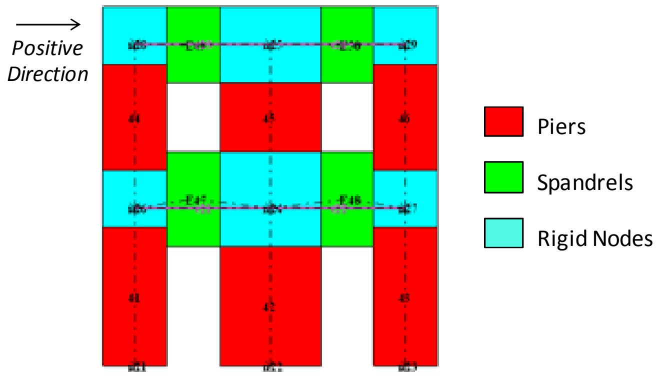

Figure 4. Equivalent frame idealisation of the masonry wall.

On the other hand, spandrels are modelled in a simpler way, as nonlinear beam elements. As such, their response is determined by stiffness, strength and ultimate displacement capacity by assuming an appropriate shear-drift relationship. In particular, the ultimate strength is computed according to simplified criteria in accordance with suggestions from the literature and modern codes (e.g. EC8 2005; Italian Code for Structural Design 2008) and with regard to different possible modes of failure (rocking, crushing, and diagonal cracking). Tie-rod elements have been modelled coupled to spandrels.

Both in the macroelement analysis as well as in the FE analysis, the elastic properties of the masonry materials were selected in such way so as to represent typical old urban construction in Italy, assuming worn cracked conditions (Young's Modulus E = 1050 MPa). Mechanical properties were assumed to be consistent with the values proposed in the Italian Code for Structural Design [2008] and are summarized in **Table 1**. Panel failure is judged in terms of drift limit values determined with respect to the prevailing failure mode. More specifically, in the case of piers, limit drift ratios of the order of 0.6% and 0.9% have been adopted for prevailing shear or flexural failure respectively. In the case of spandrels the limit drift ratio was set equal to 1.5% irrespective of the failure mechanism.

Table 1. Details of the masonry panels modelling.

Type	**Shear Strength (τ_0 : MPa)**	**Cohesion (c : MPa)**	**Friction Coef. (μ)**	**Compr. Strength (f_m : MPa)**	**Failure Criterion**
Piers	-	0.13	0.2	4	Mohr Coulomb failure criterion with c and μ values assumed representative of Diagonal Cracking failure mode [Mann and Muller, 1980]
Spandrels	0.08	-	-	4	Equivalent strut assumption due to the presence of tie-rods. Shear strength is evaluated with respect to the Turnsek and Casovic [1971].

4. FAULT RUPTURE–STRUCTURE INTERACTION: CHARACTERISTIC RESULTS

Figure 5 serves as an illustrative demonstration of the so called fault rupture–soil–foundation–structure interaction (FR-SFSI) phenomenon which is herein addressed with particular emphasis to the structure position *s* with respect to the fault. The figure portrays a set of six cross-section views of the deformed FE mesh with superimposed plastic strain contours for six different positions of the masonry wall. Plastic strain localizations indicate in every case the dominating soil failure mechanism, characterized mainly by the propagation of fault deformation but also by the soil deformation due to the displacement of the structure.

All six deformed FE mesh snapshots refer to 0.8 m of bedrock displacement. It is evident that the presence of the masonry structure on the way of the fault alters more or less the free field rupture path, the extent of this effect ranging from very limited to dramatic depending on the exact position of the structure. Minimum appears to be the deviation of the fault rupture pattern from the free field fault plane in cases A and B. Yet, as the free field fault–structure interaction point moves towards the hanging wall, and hence the fault outcrops at some position underneath the foundation base, soil failure does not localize upon a single well-defined plane but spreads into a wider zone. This is associated with either (i) diffusion of the fault deformation in a wider area under the structure body as in cases C and D or (ii) formation of secondary fault strands, which deviate from the main rupturing plane propagating with greater dip angles to outcrop off the foundation area towards the hanging wall (as in cases E and F). Domination of strikingly different fault rupture patterns for different positions of the structure naturally brings about equally important differences in its response. The latter is pointed out by the variation in the magnitude of foundation displacements (rotation θ and vertical displacement δz) illustrated in **Figure 5** for the specific fault throw magnitude (h = 0.8 m). In a few words, it may be observed that in cases A and B, where the fault crosses the structure near its left edge, the response of the structure is governed by translational movement which follows the movement of the hanging wall. By contrast, minimum rigid-body displacements are associated with positions were the fault crosses the structure near its right edge (case F) when the structure remains stationary standing almost entirely on the footwall side. Intermediate positions are characterized by a combination of translational and rotational movement and peak rotational response occurs in the range of possible positions $s \approx 1 - 2$ m.

Although the numerical study considered a greater number of possible positions, due to space limitations, the following presentation of results focuses on three characteristic possible position cases:

- s = -0.54 m, the fault rupture outcrops about 0.5 m to the left of the structure (towards the footwall)
- s = 2.1 m, the free field rupture crosses Footing 2 at its left (footwall side) corner
- s = 4.34 m, the free field rupture crosses Footing 2 at its right (hanging wall side) corner

Figure 6 compares the surface displacement profiles for these three characteristic positions to the case of fault propagation in the free field (dashed gray lines) for a range of bedrock dislocation amplitudes *h*. In the case of s = –0.54 m the structure obviously moves along with the hanging wall, standing practically on the edge of the fault crest. Its presence causes only some rather negligible difference in the soil deformation pattern with regard to the response in the free field. Contrastingly different is the case for s = 2.1 m. Here the free field fault would cross the centre footing near its middle point, but interaction mechanisms take place to drastically modify the response. Fault deformation propagates over a wide soil area, which spans the entire width of the centre footing and forms two distinct soil bulges at both door openings, where relative fault displacement takes place thanks to the reduced stress field. As a result, the structure experiences very large rotational displacements. Finally, in the case of s = 4.34 m the fault practically outcrops on the right (hanging wall side) of the structure, leaving it barely undisplaced on the footwall side. Furthermore it is worth observing the excessively nonlinear soil–foundation interface response, manifested by evident sliding and uplifting of the foundations in all three position cases.

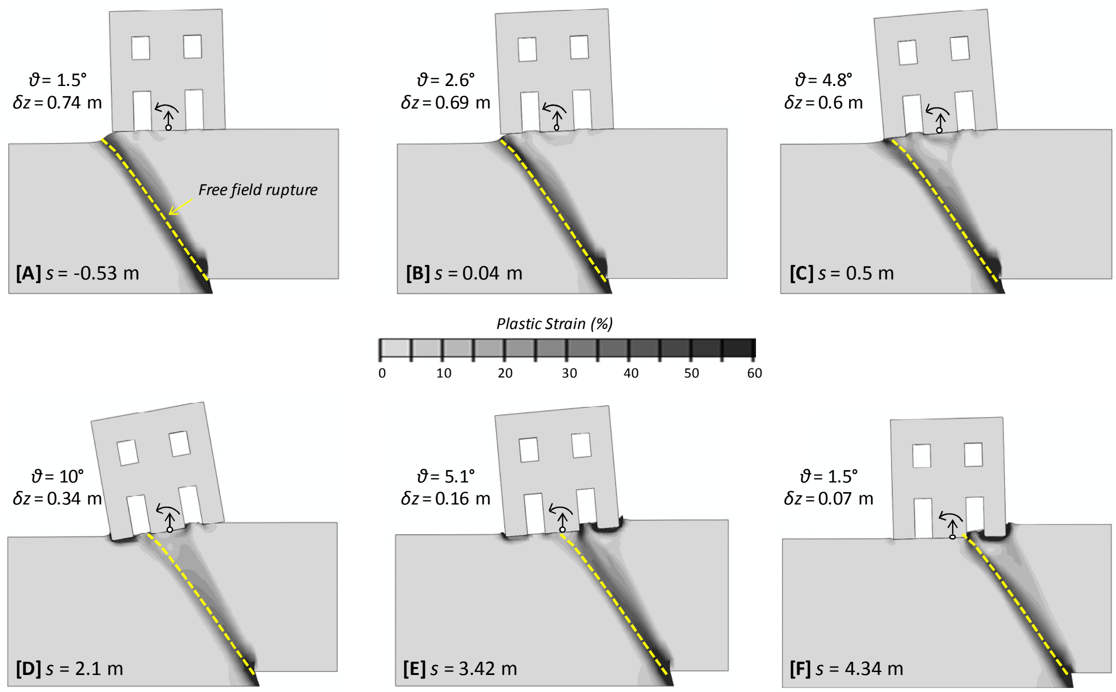

Figure 5. Fault rupture–structure interaction with respect to position parameter *s* for 0.8 m of fault throw .

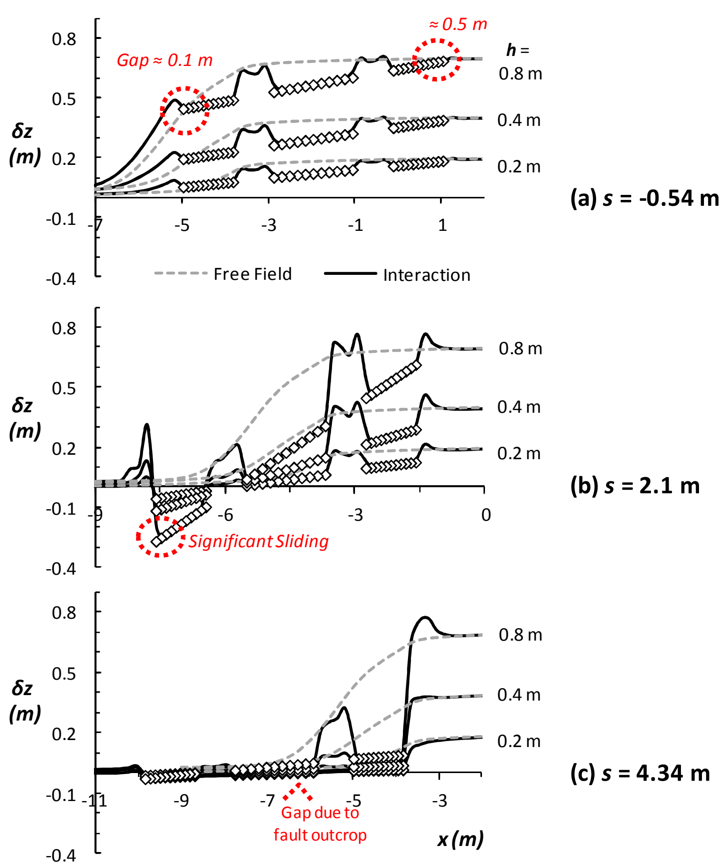

Figure 6. Surface displacement profiles for three different structure positions for a range of fault displacements.

5. VULNERABILITY ASSESMENT: COUPLING OF TECTONICWITH INERTIAL LOADS

A series of nonlinear analyses of the masonry wall were carried out pursuing the objective of assessing the effect of the previously discussed fault originated permanent ground deformations on the response of the masonry structure.

Such assessment is conducted in two steps, wherein the structure is first subjected to base displacements according to the results of the preceding FE analyses (see **Figure 6**) and then it is subjected to horizontal pushover loading, aiming to take account of the following two response parameters: (i) the masonry wall damage induced owing to the deformation of its foundation level, and (ii) the effect of this on the ability of the structure to carry lateral loads, or in other words, the effect of fault displacements to the seismic vulnerability of the structure. It should be pointed out that the second step constitutes a simplified, yet essential, attempt to couple the components of fault rupture load with the naturally associated seismic (lateral) loads. Characteristic results of this analysis are shown in the following in terms of lateral load (V) versus lateral displacement (u) pushover curves accompanied by corresponding snapshots of the deformed wall with indication of damage patterns.

For clarity, it is necessary to briefly discuss first the case where the structure is subjected to horizontal pushover loading while standing on a horizontal undeformed base, which serves as reference for comparison. **Figure 7** summarizes the results of such a loading scenario showing the response of the structure in the V–u domain with particular remarks on critical phases of response and indications of the associated wall damage. Nonlinear response of the structure is signaled by the concentration of shear stresses in the spandrels (phase a), where shear capacity is exhausted after approximately 8 mm of horizontal displacement. Conspicuously nonlinear element behaviour characterizes the response after this point, resulting in excess shearing (phase b) and failure (phase c) of the central ground floor pier. Peak lateral capacity of the structure is reached at this point ($u \approx 27$ mm) and evident strength degradation takes place thereafter. Finally, after about two times greater lateral displacement, the development of a "soft storey" mechanism leads to collapse (phase d).

Figure 8 summarizes the effect of fault rupture ground deformations on the response of the structure for the three considered characteristic positions: s = -0.54 m; 2.1 m; and 4.34 m. It should be noted that due to the assumption of elastic structural response in the FE analyses, it was considered realistic to focus on relatively small amplitude tectonic displacements which would not induce profoundly nonlinear structural response. Hence, the presented results refer to fault throws of 0.2 and 0.4 m.

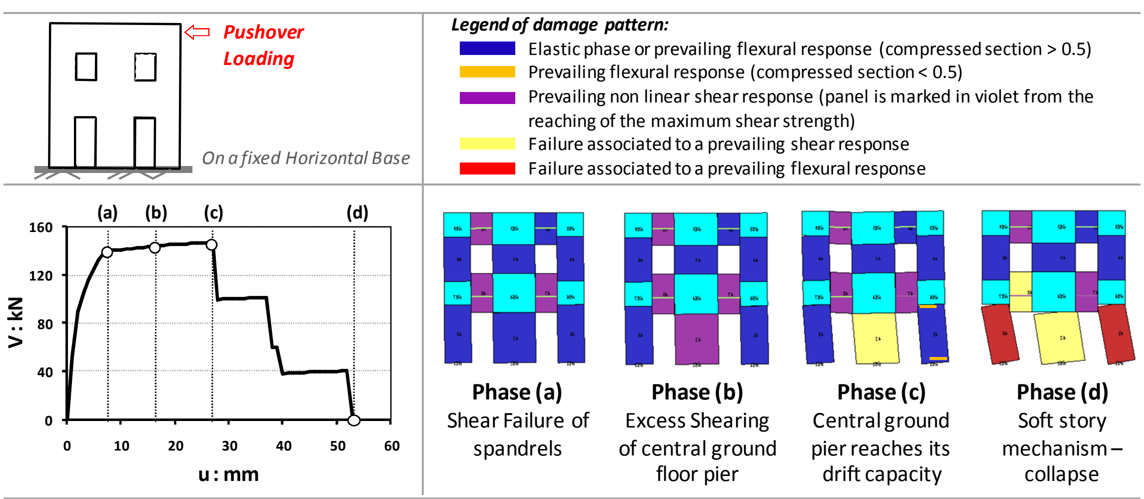

Figure 7. Lateral load (V) versus horizontal displacement (u) response and associated evolution of the wall damage for the case that the structure is *not* affected by permanent ground displacements due to fault rupture.

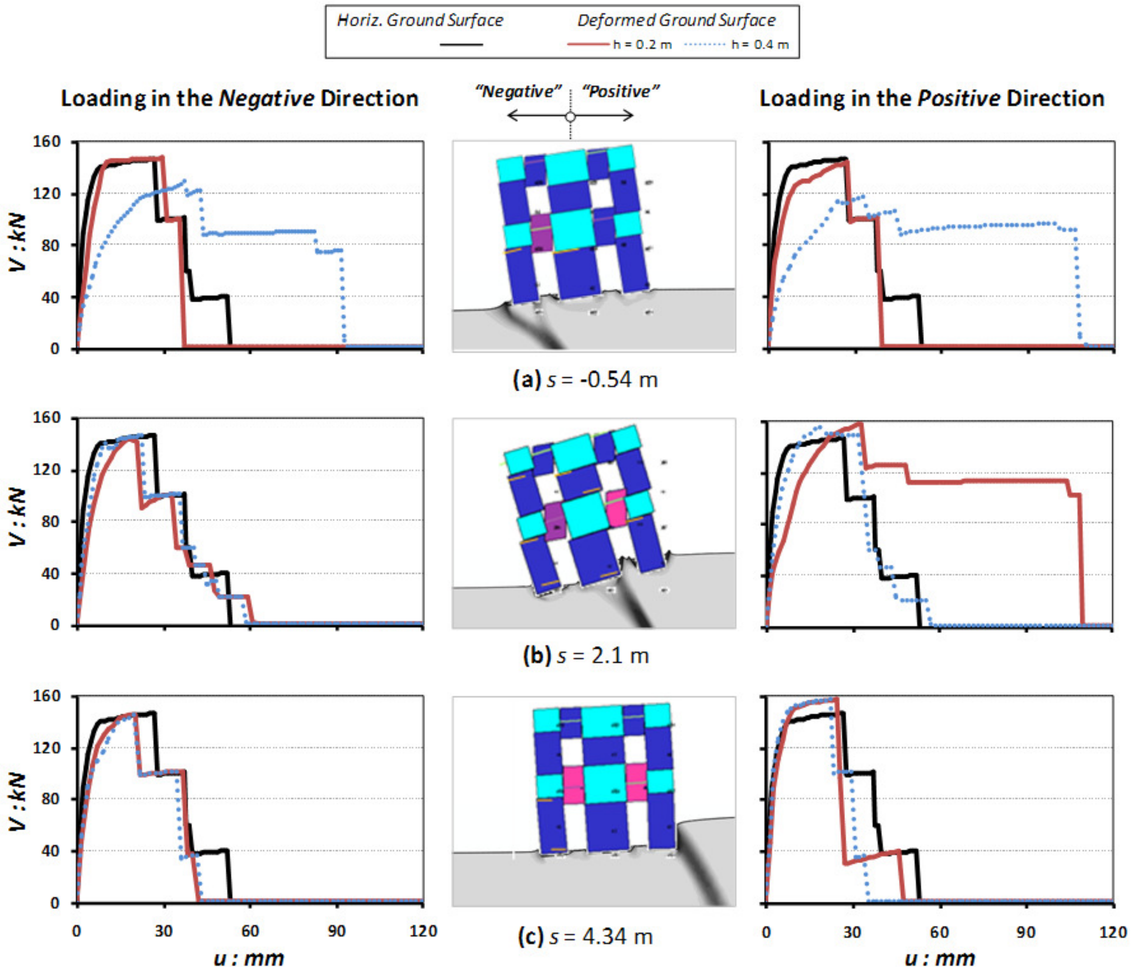

Figure 8. Effect of the fault associated permanent ground deformation on the lateral capacity of the structure.

The three illustrated schematics combine results from the FE analyses, showing in each case the prevailing interaction mechanism, with results from the equivalent frame structural analysis, indicating the amount of structural distress induced after 0.2 m of fault displacement. The indicated wall damage configuration suggests that nonlinear response does take place in all three cases, although limited to the spandrels, even for such small bedrock displacement. Characterized by shear overload of the spandrels, accompanied in some cases with considerable flexural distress in the piers, the damage pattern experienced by the wall is quite similar in all three positions, being yet evidently more intense in the case of s = 2.1 m wherein the fault outcrops just underneath the structure causing amplified foundation rotations in comparison to the other two cases.

$V - u$ plots highlight the "asymmetry" in the effect of ground displacements, comparing the response of the structure during lateral pushover loading after 0.2 m or 0.4 m of fault displacement with the benchmark scenario of undeformed base for loading in the "positive" direction (against the direction of fault displacements) or in the opposite ("negative") direction. It is interesting to observe that there is no clear trend in the effect of increasing bedrock displacement, and in some cases the response varies significantly with respect to h. Yet, it can be generally deduced that due to the damage caused by fault displacements, the stiffness is reduced in all of the investigated scenarios. Furthermore, loading in the "negative" direction consistently causes deterioration of the structure capacity, in terms of maximum load and/or ductility, in comparison to the benchmark scenario. Less straightforward appear the results for loading in the "positive" direction, as in some cases the counteracting fault deformations surprisingly lead to an increase in the maximum lateral load capacity of the structure.

6. CONCLUSIONS AND LIMITATIONS

The paper has presented a newly developed hybrid methodology for the analysis and assessment of the vulnerability of historic masonry structures to tectonic permanent ground displacements. This involves two steps, whereby a validated 3D nonlinear FE method is used for the prediction of the surface ground displacements and the associated displacement load imposed onto the structure, the later being thereafter used as input in a nonlinear equivalent frame model of the structure, wherein the various attributes of nonlinear masonry wall response are thoroughly taken into account. The nonlinear structural model is used not only for estimation of the fault induced wall damage but also for prediction of the effect of this damage on the ability of the structure to carry lateral loads, i.e. its seismic vulnerability. Results have provided valuable insights on the different mechanisms of fault–soil–structure interaction and their manifold and "asymmetric" impact on the response of the overlying structure.

It is important to highlight the main limitation of the presented methodology, which refers to the assumption of elastic superstructural response in the FE analysis, and may have lead to underestimation of the fault induced damage in the wall. Effort is currently put into improving this methodology by incorporating a simplified nonlinear model of the wall behaviour in the FE method, aiming at providing an efficient tool for the assessment of tectonic risk in historic structures.

AKCNOWLEDGEMENT
The results have been achieved in the project PERPETUATE (www.perpetuate.eu), funded by the European Commission in the Seventh Framework Programme (FP7/2007-2013), under grant agreement n° 244229".

REFERENCES

Anastasopoulos I. & Gazetas G. (2007), "Foundation-Structure Systems over a Rupturing Normal Fault : Part I. Observations after the Kocaeli 1999 Earthquake", *Bulletin of Earthquake Engineering*, **5:3**, 253–275.

Anastasopoulos I., Gazetas G., Bransby M.F., Davies M.C.R., and El Nahas A. (2007), "Fault Rupture Propagation through Sand : Finite Element Analysis and Validation through Centrifuge Experiments", *Journal of Geotechnical and Geoenvironmental Engineering*, ASCE, **133:8**, 943–958.

Anastasopoulos I., Gazetas G., Bransby M.F., Davies M.C.R., and El Nahas A. (2009), "Normal Fault Rupture Interaction with Strip Foundations", *Journal of Geotechnical and Geoenvironmental Engineering*, ASCE, **135:3**,359-370.

Bray J.D., Seed R.B., Cluff L.S., Seed H.B. (1994b), "Analysis of earthquake fault rupture propagation through cohesive soil", *Journal of Geotechnical Engineering*, ASCE, **120:3,** 562-580.

Eurocode 8- Part 3 (2005), Design of structures for earthquake resistance. ENV 1998-3, CEN: Brussels, 2005.

Galasco A., Lagomarsino S., Penna A. and Cattari S. (2009), TREMURI program: Seismic Analyses of 3D Masonry Buildings, University of Genoa (mailto:tremuri@gmail.com).

Galasco, A., Lagomarsino S., Penna, A., Resemini, S. (2004), "Non-linear seismic analysis of masonry structures", *Proc. 13th WCEE*, Vancouver, paper n.843.

Gambarotta, L., Lagomarsino, S., 1997, "Damage models for the seismic response of brick masonry shear walls, Part II: the continuum model and its applications", *Earthquake Engineering and Structural Dynamics*, **26**.

Italian Code for Structural Design (2008), D.M. 14/1/2008, Official Bullettin no. 29 of 4/02/2008 (In Italian).

Loli, M. Anastasopoulos, I. Bransby, M.F. Ahmed, W. Gazetas, G. (2010) "Caisson Foundations subjected to Reverse Fault Rupture: Centrifuge Testing and Numerical Analysis." *Journal of Geotechnical and Geoenvironmental Engineering*, ASCE, **137:10**,914–925.

Magenes G., Kingsley G.R., and Calvi G.M. (1995), "Seismic Testing of a Full-Scale, Two-Story Masonry Building: Test Procedure and Measured Experimental Response," *Experimental and numerical investigation on a brick masonry building prototype* , CNR-GNDT, pp.1- 41.

Mann, W. and Müller, H. (1980), "Failure of shear-stressed masonry – An enlarged theory, tests and application to shear-walls", *Proc. of the International Symposium on Loadbearing Brickwork*, London, 1980; 1-13.

Penna A. (2002), "A macro-element procedure for the non-linear dynamic analysis of masonry buildings", Ph.D. Dissertation (in italian), Politecnico di Milano, Italy.

Turnšek, V. and Čačovič, F. (1970)," Some experimental results on the strength of brick masonry walls". *Proceedings of the 2nd International Brick Masonry Conference*, Stoke-on-Trent, 149-156.